



Nanosized $\text{Li}_4\text{Ti}_5\text{O}_{12}$ Prepared by Molten Salt Method as an Electrode Material for Hybrid Electrochemical Supercapacitors

Liang Cheng, Hai-Jing Liu, Jing-Jun Zhang,
Huan-Ming Xiong, and Yong-Yao Xia^{*,z}

Department of Chemistry and Shanghai Key Laboratory of Molecular Catalysis and Innovative Materials,
Fudan University, Shanghai 200433, China

Nanosized lithium titanium oxide ($\text{Li}_4\text{Ti}_5\text{O}_{12}$) powder has been prepared using LiCl as a high-temperature flux. X-ray diffraction, scanning electron microscope, and transmission electron microscope measurements indicate that the obtained $\text{Li}_4\text{Ti}_5\text{O}_{12}$ particles are uniform and the particle size of $\text{Li}_4\text{Ti}_5\text{O}_{12}$ powder can be controlled by flux content and heating time. Under the optimal synthetic condition, the particle-size distribution is narrow (~ 100 nm). The hybrid electrochemical supercapacitors using a nanosized $\text{Li}_4\text{Ti}_5\text{O}_{12}$ negative electrode in combination with an activated carbon positive electrode show much better rate capability than those based on the conventional $\text{Li}_4\text{Ti}_5\text{O}_{12}$ prepared by solid-state reaction.
© 2006 The Electrochemical Society. [DOI: 10.1149/1.2204872] All rights reserved.

Manuscript submitted January 11, 2006; revised manuscript received March 28, 2006. Available electronically June 5, 2006.

Li-ion intercalated compound $\text{Li}_4\text{Ti}_5\text{O}_{12}$ (LTO) has an excellent Li-ion insertion/extraction reversibility and exhibits no structural change (zero-strain insertion material) during charge–discharge cycling.^{1–8} Recently, spinel $\text{Li}_4\text{Ti}_5\text{O}_{12}$ has been demonstrated as the most promising electrode materials used for hybrid electrochemical supercapacitors which typically consist of an electrochemical double-layer capacitor (EDLC) electrode and a battery electrode.^{9,10} In the hybrid system, both increase of the working voltage and high energy density of the negative result in a significant increase of the overall energy density of the capacitors. Accordingly, the energy density of the capacitor is critically dependent on the energy density of the carbon positive electrode material and the cell working voltage, but the power density depends on the rate capability of the intercalated compound which is associated with the Li-ion diffusion coefficient and the diffusion distance in the intercalated compound particle.¹¹ To obtain a high rate capability, it is necessary to develop a nanosized $\text{Li}_4\text{Ti}_5\text{O}_{12}$ material. For most Li-ion intercalated compounds, e.g., LiMn_2O_4 , LiCoO_2 , it is easy to obtain the nanosized particles by a sol-gel method or pechini process in which citric acid and polyethylene glycol are added.^{12–14} In such cases, lithium and transition metal cations are normally trapped homogeneously on atomic scale throughout a polymer matrix, and thus the reaction temperature and time are reduced. However, it is hard to obtain $\text{Li}_4\text{Ti}_5\text{O}_{12}$ through these methods because most of titanium salts, the starting precursors are easily hydrolyzed to form TiO_2 . Once TiO_2 is formed, it is necessary to calcine it with lithium salts (Li_2CO_3 or LiOH) at high temperature (750°C or above) for a long time in order to obtain well crystallized $\text{Li}_4\text{Ti}_5\text{O}_{12}$. As a result, the particle size ranges from several hundred nanometers to several micrometers. To date, the nanosized $\text{Li}_4\text{Ti}_5\text{O}_{12}$ with outstanding electrochemical characters can only be obtained by spray pyrolysis,¹⁵ but no simple chemical method has been reported to prepare the nanosized grain of LTO with excellent electrochemical characters.

Now, a molten salt process has been used in synthesizing electrode materials.^{16–19} In the present work, we use LiCl as a high-temperature flux to prepare the uniform nanosized particles of spinel $\text{Li}_4\text{Ti}_5\text{O}_{12}$ from TiO_2 and Li_2CO_3 for the first time. The effects of the molar ratio of LiCl to reaction precursor, heat-treatment temperature, and time on the particle size, as well as the electrochemical profile used as the electrode material for hybrid supercapacitors were extensively investigated.

Experimental

In this work, we prepared $\text{Li}_4\text{Ti}_5\text{O}_{12}$ by the solid-state reaction process (SS process) and the molten salt synthesis process (MS process). Anatase titanium dioxide (TiO_2) with the particle size of 8 nm was used as titanium source (Zhoushan Mingri Chemical Co.); Li_2CO_3 was used as the lithium source. In the solid-state reaction process, anatase type TiO_2 and Li_2CO_3 with the molar ratio of 5/2 were mixed well. Then, the mixture was heated at various temperatures from 700 to 750°C for different treating times, and cooled to obtain the final product.

The difference of the molten salt synthesis process from the conventional solid-state reaction process was using LiCl as the high-temperature flux. The different contents of LiCl (N) was mixed with TiO_2 and Li_2CO_3 in which N was defined as the molar ratio of LiCl/TiO_2 , and N varies from 2/1 to 16/1. Then, the precursor was also heated at different temperatures for different time periods. The products were immersed in deionized water, washed, and filtered to remove the residual fluxes. Finally, the products were dried at 120°C for 24 h.

The phase composition of the obtained compounds was identified by X-ray diffraction (XRD, Bruker D8 X-ray diffractometer) with Cu K α radiation. The scan data for the Rietveld refinements were collected between 10 to 90° with a step interval of 0.015° and graphite was added to some of the products as an indicator for data modification. Structural refinements were carried out with a Rietveld refinement program RIETAN-2000. The morphologies and particle sizes were characterized with scanning electron microscopy (SEM) in a Philips XL-60 scanning microscope and transmission electron microscope (TEM, JOEL JEM2010). Nitrogen adsorption-desorption isotherms of the product $\text{Li}_4\text{Ti}_5\text{O}_{12}$ were measured at 77 K on Micromeritics Co. Ltd., Tristar. The total specific area was determined by the multipoint Braunauer-Emmett-Teller (BET) method.

The $\text{Li}_4\text{Ti}_5\text{O}_{12}$ electrode was prepared by mixing 65% active material, 25% carbon black, and 10% poly(tetrafluoroethylene) (PTFE) dispersed in isopropanol. The slurry was pressed onto a current collector and punched to a disk of $\varphi = 12$ mm. The activated carbon electrode was prepared by the same process except that the slurry was made of 85% active material, 10% carbon black, and 5% PTFE dispersed in isopropanol. Then the $\text{Li}_4\text{Ti}_5\text{O}_{12}$ and the activated carbon electrodes were dried in a vacuum oven at 80°C for 12 h to remove the solvent. The electrochemical tests were taken on a coin-type cell (CR2016) assembled with positive electrode/separator/negative electrode in an argon filled glove box. For the half cell test, the $\text{Li}_4\text{Ti}_5\text{O}_{12}$ electrode was assembled with lithium metal negative electrode. As to the hybrid supercapacitor assembling, the activated carbon electrode was used as the positive and the

* Electrochemical Society Active Member.

^z E-mail: yyxia@fudan.edu.cn

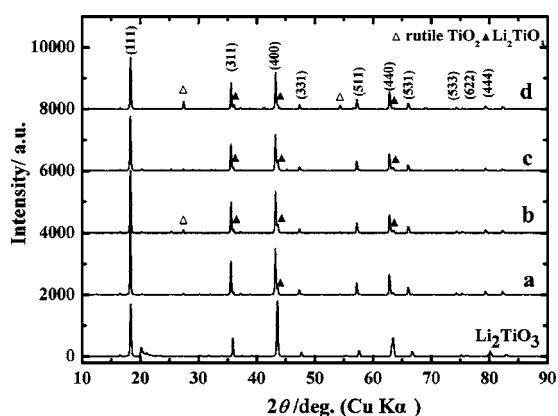


Figure 1. XRD patterns of $\text{Li}_4\text{Ti}_5\text{O}_{12}$ samples prepared by solid-state reaction process. (Δ) peak of rutile TiO_2 , (\blacktriangle) peak of Li_2TiO_3 . (a) 750°C-12 h, (b) 750°C-4 h, (c) 700°C-12 h, and (d) 700°C-4 h.

$\text{Li}_4\text{Ti}_5\text{O}_{12}$ electrode as the negative and the typical active material mass load of negative electrode material is 5 and 15 mg/cm^2 for the positive electrode according to our electrochemical test results. The electrolyte was a 1 M LiPF_6 ethylene carbonate (EC)/ethylene methyl carbonate (EMC)/dimethyl carbonate (DMC) (1:1:1 in volume).

Results and Discussions

Characterizations of $\text{Li}_4\text{Ti}_5\text{O}_{12}$ prepared by a solid state reaction.—To obtain the well crystallized $\text{Li}_4\text{Ti}_5\text{O}_{12}$ with a finer electrochemical performance, the necessary reaction temperature and the minimum heating time of $\text{Li}_4\text{Ti}_5\text{O}_{12}$ formation from a solid state reaction of TiO_2 and Li_2CO_3 was first investigated (SS process). Figure 1 shows the XRD patterns of $\text{Li}_4\text{Ti}_5\text{O}_{12}$ prepared at various temperatures and treating time. The results in Fig. 1 reveal that all resulting products show very similar XRD patterns. The major diffraction peaks at 2θ equal 18.4, 35.6, 43.3, 47.4, 57.2, 62.8, 66.1, 74.3, 75.4, and 79.4° were found. The product can be indexed to spinel structure $\text{Li}_4\text{Ti}_5\text{O}_{12}$.^{1,2} However, all products contain small amount of Li_2TiO_3 the rock salt structure Li_2TiO_3 (which has peaks at 2θ : 18.6, 36.2, 43.7, 57.9, 63.5, and 67.0°) were found. For the samples prepared at temperature below 750°C and/or short times, it

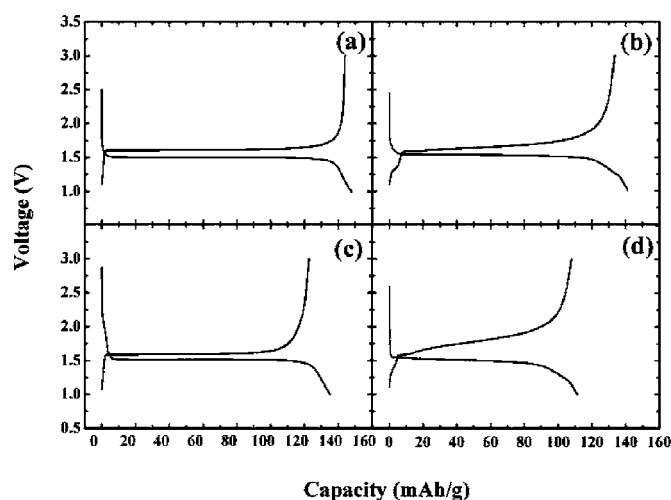


Figure 2. Electrochemical performance of $\text{Li}_4\text{Ti}_5\text{O}_{12}$ samples prepared by solid-state reaction process. The cell was charge/discharge at a current rate of 0.2 mA/cm^2 between 1.0 and 3.0 V. (a) 750°C-12 h, (b) 750°C-4 h, (c) 700°C-12 h, and (d) 700°C-4 h.

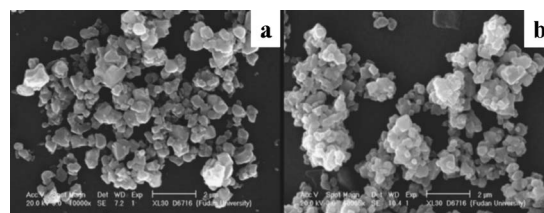


Figure 3. SEM of $\text{Li}_4\text{Ti}_5\text{O}_{12}$ samples prepared at different heat-treatment temperatures for 12 h using a solid-state reaction process, (a) 750° and (b) 700°C.

also contains unreacted rutile TiO_2 phases which has peaks at 2θ : 27.5, 36.0 and 54.2°. All results suggest that both compounds have a significant possibility of being formed as impurities, and it is difficult to achieve a single-phase $\text{Li}_4\text{Ti}_5\text{O}_{12}$ by the conventional solid-state reaction process.

The above four samples were characterized by constant current charge/discharge tests at a current rate of 0.2 mA/cm^2 (40 mA/g) between 1.0 and 3.0 V. Typical charge/discharge curves are shown in Fig. 2. Sample SS-a gives a discharge capacity of 151 mAh/g , which is the highest among the four samples. The discharge capacity decreases as the decreasing of temperature and/or time. The first discharge capacities were 141, 140, and 116 mAh/g for samples SS-b, SS-c, and SS-d, respectively. Moreover, sample SS-a shows a very flat discharge plateau at about 1.5 V and the charge voltage is 1.6 V (vs Li^+/Li), however samples SS-b and SS-d (prepared at low temperature or short time) deliver sloping charge/discharge curves which is consistent with that prepared by the thermhydro method at low temperature reported by Zhang et al.²³ The difference in charge/discharge profile is mostly correlative to its crystal structure. It may be due to the formation of defect spinel structure at low temperature and short time during annealing process, which should be further clarified. Figure 3 gives the SEM observation of $\text{Li}_4\text{Ti}_5\text{O}_{12}$ prepared at 750 and 700°C for 12 h. The average particle size was ~ 700 nm.

From the above results, we can conclude that it is necessary to prepare $\text{Li}_4\text{Ti}_5\text{O}_{12}$ at a relatively high temperature for a relatively long time to obtain a better electrochemical performance. Therefore, the optimal treating condition of conventional solid state reaction in our experiment is set to 750°C-12 h. However, these treatment conditions result in a relatively large particle size (ca. 700 nm) or larger than. Although it can be used as the negative electrode material in

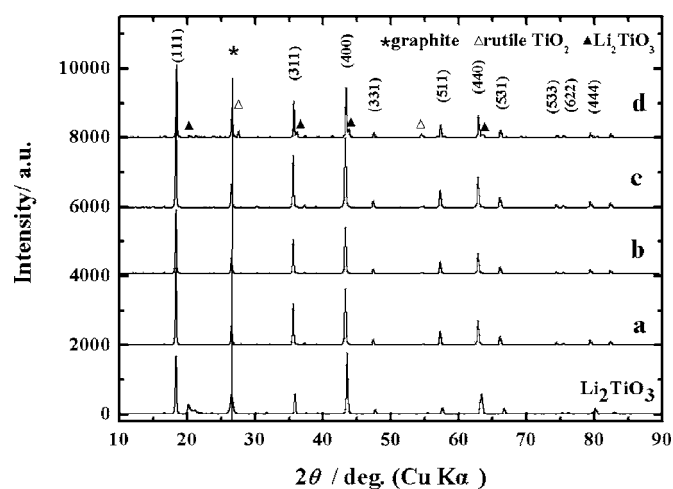


Figure 4. XRD patterns of $\text{Li}_4\text{Ti}_5\text{O}_{12}$ samples prepared by a molten-salt reaction process with a molar ratio of LiCl/TiO_2 of 16. (Δ) peak of rutile TiO_2 , (\blacktriangle) peak of Li_2TiO_3 , (*) graphite served as a reference sample, (a) 750°C-12 h, (b) 750°C-1 h, (c) 700°C-12 h, and (d) 700°C-1 h.

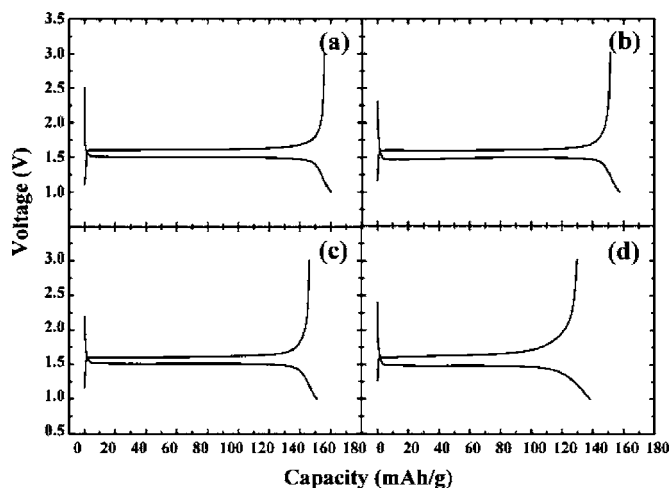


Figure 5. Typical charge/discharge profiles of four compounds synthesized by a molten-salt reaction process with a molar ratio of LiCl/TiO_2 of 16. The cell was charge/discharge at a current rate of $0.2 \text{ mA}/\text{cm}^2$ between 1.0 and 3.0 V. (a) 750°C -12 h, (b) 750°C -1 h, (c) 700°C -12 h, and (d) 700°C -1 h.

the asymmetric hybrid nonaqueous supercapacitor, the particle size is not small enough to satisfy the high rate requirement.

$\text{Li}_4\text{Ti}_5\text{O}_{12}$ prepared by a molten salt process.— The particle size of the precursor TiO_2 is $\sim 8 \text{ nm}$; however, it becomes 700 nm during heat-treatment. It is most likely due to the particle agglomeration due to heat-treatment at relative high temperature and long time. To overcome this problem, we herein prepared a series of $\text{Li}_4\text{Ti}_5\text{O}_{12}$ by using LiCl as a high-temperature flux (MS process). For comparison with the solid-state reaction synthesized $\text{Li}_4\text{Ti}_5\text{O}_{12}$, the starting materials are also anatase TiO_2 and Li_2CO_3 except the addition of LiCl flux, and the synthesis condition was first set at 750°C for 12 h (sample refers to MS-a), and then reduced time to 1 h (sample refers to MS-b), further also reduced the heating temperature at 700°C for 12 h (sample refers to MS-c) and 1 h (sample refers to MS-d). The molar ratio of $\text{LiCl}:\text{TiO}_2$ is set to 16:1 ($N = 16$) which can be the extreme, and the effect of the molar ratio of LiCl flux is discussed later in the paper.

XRD patterns of all four samples shown in Fig. 4 reveal that the resulting compounds can be considered as single-phase spinel structure $\text{Li}_4\text{Ti}_5\text{O}_{12}$ except sample MS-d, which contains some impuri-

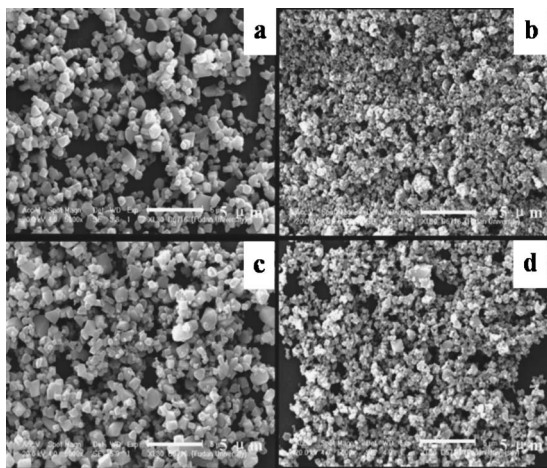


Figure 6. SEM of four $\text{Li}_4\text{Ti}_5\text{O}_{12}$ compounds prepared by MS process with molar ratio of LiCl/TiO_2 of 16. (a) 750°C -12 h, (b) 750°C -1 h, (c) 700°C -12 h, and (d) 700°C -1 h.

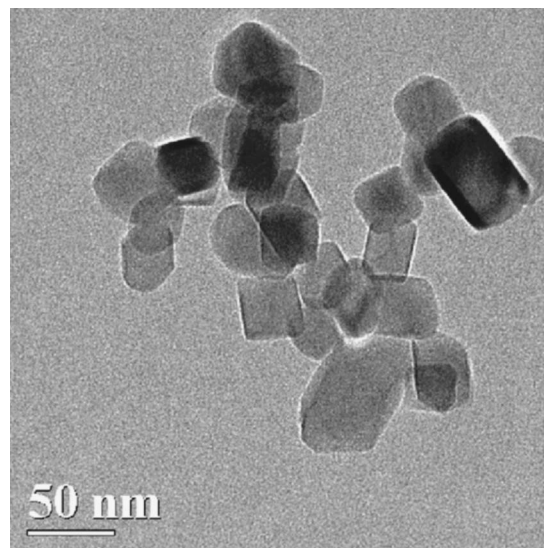


Figure 7. TEM of $\text{Li}_4\text{Ti}_5\text{O}_{12}$ compound prepared by MS process at 750°C for 1 h with a molar ratio of LiCl/TiO_2 of 16.

ties. Figure 5 shows the typical charge/discharge profiles of above four compounds at a current rate of $0.2 \text{ mA}/\text{cm}^2$ ($40 \text{ mA}/\text{g}$) between 1.0 and 3.0 V. Very similar charge/discharge behaviors were observed for the samples prepared by MS process and that by the SS process. The greatest differences between the compounds prepared by two different processes are that the capacities of compounds by the conventional MS process method are higher than that synthesized by SS process under the same treatment conditions. The discharge capacities are 161, 159, 152, and 140 mAh/g for the compound MS-a, MS-b, MS-c, and MS-d, respectively. In Fig. 6 we compare the SEM images of the above four compounds prepared by MS process with the compound prepared by SS process at 750°C for 12 h (SS-a). The SEM observations clearly indicate that the difference in the particle size was barely detectable for the compounds prepared by MS process and SS process at 750°C for 12 h, both compounds have the average particle size $\sim 700 \text{ nm}$, while the compounds prepared by MS process for 1 h only show a particle size of ca. 100 nm with a clearer TEM image in Fig. 7. The findings suggest that the flux LiCl accelerates the formation of $\text{Li}_4\text{Ti}_5\text{O}_{12}$ within a short time, thus preventing the particle from agglomerating. It is most interesting that the compound treated at 750°C only for 1 h shows an outstanding capacity of 159 mAh/g, which is similar to that of the compound SS- 750°C -12 h. To shed some light on this issue, we employed the Rietveld method,²⁴⁻²⁶ to analyze the crystal structure of the compounds MS- 750°C -1 h, SS- 750°C -12 h, MS- 750°C -12 h. 5333 data points were collected between $2\theta = 10^\circ$ - 90° with a step interval of 0.015° . A simultaneous refinement was carried out on the stoichiometric spinel phase $\text{Li}[\text{Li}_{0.33}\text{Ti}_{1.67}]\text{O}_4$ (space group $Fd3m$, no. 227). We only fixed the oxygen occupation and allowed additional lithium on 16d sites. Both titanium and lithium occupation in the 8a and 16d sites were allowed to vary. The crystallographic parameters are listed in Table I. $\text{Li}_4\text{Ti}_5\text{O}_{12}$ has a cubic spinel structure and the lattice constant is 8.368 \AA .⁸ Our

Table I. Crystallographic parameters of $\text{Li}_4\text{Ti}_5\text{O}_{12}$ prepared by MS and SS process.

	MS- 750°C -1 h, $N = 16$	MS- 750°C -12 h, $N = 16$	SS- 750°C -12 h
$a = b = c$ (\AA)	8.348	8.353	8.350
R_{wp}	11.50%	11.42%	11.52%
R_p	7.95%	8.03%	8.11%

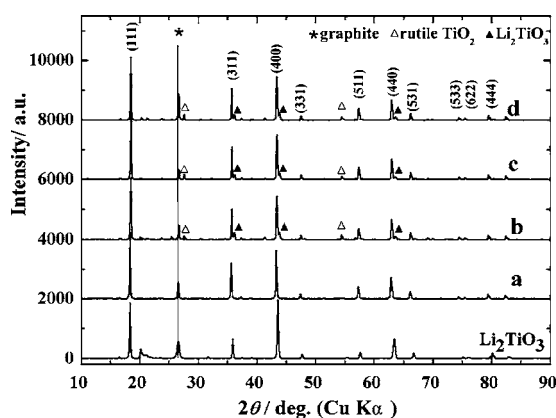
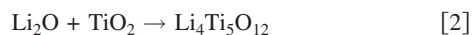


Figure 8. XRD patterns of the $\text{Li}_4\text{Ti}_5\text{O}_{12}$ powders heating at 750°C for 1 h with different LiCl contents (N , the molar ratio of LiCl/TiO_2). (Δ) peak of rutile TiO_2 , (\blacktriangle) peak of Li_2TiO_3 , (*) graphite served as a reference sample. (a) $N = 16$, (b) $N = 8$, (c) $N = 4$, and (d) $N = 2$.

results demonstrated that the LiCl-flux method gives a well-crystallized $\text{Li}_4\text{Ti}_5\text{O}_{12}$ powder within a short time.

In the view of the solid state reaction mechanism, it is well known that the formation of the resulting compounds result from the cations/anions diffusing each other in the solid matrix, and it is critically dependent on their contact area and particle size. For TiO_2 - Li_2CO_3 system, the spinel structure $\text{Li}_4\text{Ti}_5\text{O}_{12}$ was formed at temperature over 700°C . Simultaneously with the formation of $\text{Li}_4\text{Ti}_5\text{O}_{12}$, the decomposition of Li_2CO_3 into Li_2O occurred, and the total reaction in the Li_2CO_3 flux may be expressed as



In the Li_2CO_3 -LiCl flux, it is easy to form Li containing flux as LiCl has a low melting point compared with Li_2CO_3 and Li_2O . The liquid/solid interface provides a large effective reaction area, and thus accelerates the $\text{Li}_4\text{Ti}_5\text{O}_{12}$ growth at a relatively short time and the reaction can be described as



where LiCl only plays a role as a flux, and does not provide the Li source to form the $\text{Li}_4\text{Ti}_5\text{O}_{12}$ in an inert atmosphere, which is different from the case of the reaction of MnOOH and LiCl flux in which a low Mn valence LiMnO_2 was formed via a lithiation reaction.¹⁷

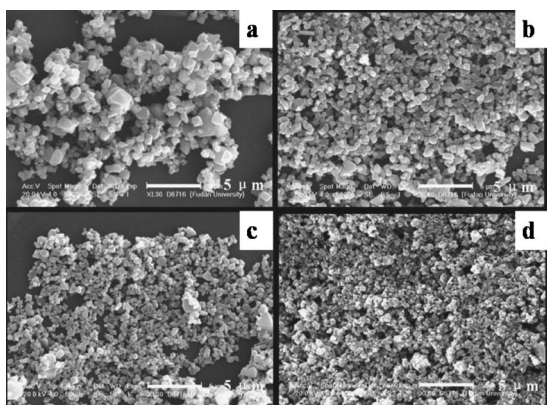


Figure 9. SEM of four $\text{Li}_4\text{Ti}_5\text{O}_{12}$ compounds heated at 750°C for 1 h by MS process with different LiCl contents (N , the molar ratio of LiCl/TiO_2). (a) $N = 2$, (b) $N = 4$, (c) $N = 8$, and (d) $N = 16$.

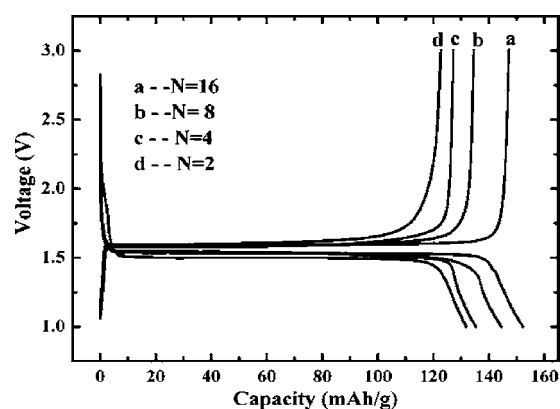


Figure 10. Typical charge/discharge curves of $\text{Li}_4\text{Ti}_5\text{O}_{12}$ compounds prepared at 750°C for 1 h with different LiCl contents (N , the molar ratio of LiCl/TiO_2). (a) $N = 16$, (b) $N = 8$, (c) $N = 4$, and (d) $N = 2$. The cell was charge/discharge at a current rate of $0.2 \text{ mA}/\text{cm}^2$ between 1.0 and 3.0 V.

Effects of the LiCl flux ratio.— We also examined the effect of molar ratio of LiCl flux and TiO_2 (N from 2 to 16) on the particle size and the electrochemical profile. Figure 8 shows the XRD patterns of the powder heating at 750°C for 1 h using different amounts of LiCl. The diffraction patterns indicate that the crystal system is identical to that of single-phase $\text{Li}_4\text{Ti}_5\text{O}_{12}$ for $N = 16$, but some impurity peaks associated with the TiO_2 and Li_2TiO_3 were detected in the other three samples. Figure 9 compares the SEM images of four compounds prepared by MS process with different ratio of LiCl flux. The SEM observations clearly indicate that the particle size varies with the LiCl flux content, it decreases from 700 to 100 nm when N increases from 2 to 16. The presence of molten salt LiCl phase probably facilitates the formation of the $\text{Li}_4\text{Ti}_5\text{O}_{12}$ phase and also prevents agglomerating of the particle. Because the diffusion rates of the components in molten salts are much higher than those in the solid-state reaction.

Typical charge/discharge curves of four compounds prepared with different LiCl flux contents of N are shown in Fig. 10. The data were obtained at a current rate of $0.2 \text{ mA}/\text{cm}^2$ ($40 \text{ mA}/\text{g}$) between 1.0 and 3.0 V. The discharge capacities decrease from 159 to 120 mAh/g when the LiCl flux contents, N , decrease from 16 to 2. Note that all compounds deliver a very flat discharge plateau at $\sim 1.5 \text{ V}$ and the charge voltage is 1.6 V (vs Li^+/Li), which is different from the sloping charge/discharge curves of these compounds prepared by SS process at low temperature of 700°C , even both the compound prepared by MS process at low LiCl flux content and the compound prepared by SS process at low temperature deliver smaller capacity and contain the same impurities. All of these indicate that the LiCl flux contents scarcely affect the crystallinity of $\text{Li}_4\text{Ti}_5\text{O}_{12}$ which was confirmed to have the same crystal structure by the Rietveld analysis; the difference in the discharge capacity is mainly due to its impurity contents as shown in the XRD patterns.

Rate capability of the hybrid supercapacitors.— Table II sum-

Table II. BET surfaces of the $\text{Li}_4\text{Ti}_5\text{O}_{12}$ materials.

Sample	Preparative notes	$S_{\text{BET}}(\text{m}^2/\text{g})$	$d(\text{nm})$
1	SS- 700°C -12 h	2.83	700
2	SS- 750°C -12 h	2.51	700
3	MS- 750°C -12 h, $N = 16$	1.62	700
4	MS- 700°C -12 h, $N = 16$	2.20	700
5	MS- 750°C -1 h, $N = 2$	3.66	650
6	MS- 750°C -1 h, $N = 4$	5.00	400
7	MS- 750°C -1 h, $N = 8$	8.15	200
8	MS- 750°C -1 h, $N = 16$	13.10	100

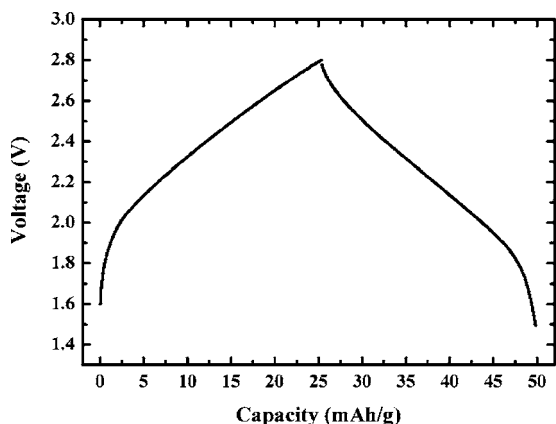


Figure 11. Typical charge/discharge curve of AC/Li₄Ti₅O₁₂ hybrid capacitor. The cell was charge/discharge at a current rate of 1.5 mA/cm² between 1.5 and 2.8 V.

marizes the surface area, S_{BET} , and particle size, d , of all Li₄Ti₅O₁₂ materials with qualified electrochemical performances. The S_{BET} was determined from nitrogen adsorption isotherm, and particle size d was estimated from the SEM observation. Sample SS-700°C-12 h and SS-750°C-12 h were synthesized by a solid state reaction process. The BET surfaces of the 6 samples range from 1.62 to 13.10 m²/g. It can be concluded from the BET data that the presence of molten salt LiCl probably facilitates the formation of the Li₄Ti₅O₁₂ and also prevents agglomerating of the particle. The rate capability of the Li₄Ti₅O₁₂ with different particle sizes was further examined in a hybrid cell in combination with an activated carbon (AC) positive electrode. The positive and negative electrodes were based on an active material weight ratio of 3:1. The balancing ratio was calculated using 30 mAh/g specific capacity for the activated carbon and 90 mAh/g specific capacity for Li₄Ti₅O₁₂. Figure 11 shows the typical charge/discharge curve of the AC/Li₄Ti₅O₁₂ hybrid capacitor of fifth cycle. The capacitor was tested from the voltage 1.5-2.8 V at a charge/discharge current rate of 1.5 mA/cm² (3C). The capacity given in the figure is calculated based on the total weight of the electrode active materials, including the positive and negative. The cell shows an average working voltage of 2.15 V. The comparisons of the discharge capacity for three samples with different particle size at different current rates are given in Fig. 12. Samples SS-750°C-12 h (750°C, 12 h) with a particle size of 700 nm, sample MS-750°C-12 h (750°C, 12 h) with

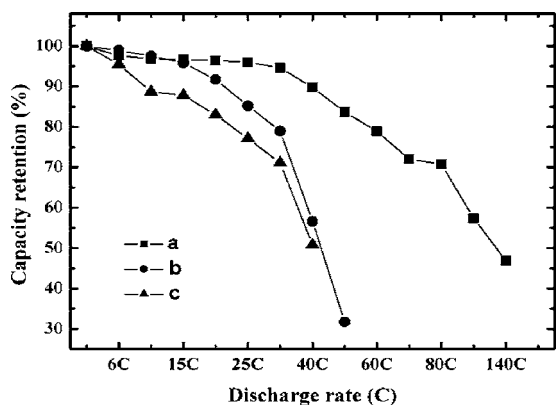


Figure 12. Rate capabilities of AC/Li₄Ti₅O₁₂ hybrid cells. Li₄Ti₅O₁₂ was prepared under different conditions with different particle sizes. (a) MS-750°C-1 h, $N = 16$, (b) SS-750°C-12 h, $N = 16$. The cell was charged at a current rate of 1.5 mA/cm² (3C) and discharged at various current rates varying from 3 to 140 C.

a particle size of 700 nm, and sample MS-750°C-1 h (750°C, 1 h) with a particle size of 100 nm were examined. The hybrid cells were charged at 1.5 mA/cm² (3C) and discharged at current rates varying from 1.5 mA/cm² (3C) to 70 mA/cm² (140C) between 1.5 and 2.8 V. The capacity retention was defined by the capacity of the hybrid cell at various current rates vs that at 3C rate. Sample MS-a-1 h with small particle size shows much better rate capability, even at 100 C discharge rate, the hybrid capacitor also keeps 60% of capacity compared with 3C discharge rate. As noted above, for the hybrid supercapacitors, the rate capability is determined by that of Li-ion intercalated compound. The electrochemical performance of a cell is mainly governed by Li⁺ diffusion length and diffusion coefficient. Diffusion length depends on particle microstructure and particle size. The smaller particles promote shorter pathways for solid-state diffusion of Li ions and result in better rate capability.^{11,26}

Conclusion

We presented a technology to prepare the nanosized lithium intercalated compound Li₄Ti₅O₁₂ by using LiCl as a high-temperature flux. Li₄Ti₅O₁₂ powders were easily obtained with homogeneity, regular morphology, and narrow particle-size distribution using molten LiCl as a high-temperature solvent. The flux produces a liquid/solid reaction interface, thus providing a large effective reaction area, and accelerates the Li₄Ti₅O₁₂ growth at a relatively short time. The particles size decreases and the distribution becomes narrow with the increasing flux content. Under the optimal synthetic condition (750°C for 1 h, $N = 16$), the average particle size is of 100 nm and the sample has a discharge capacity of 159 mAh/g. The hybrid capacitor fabricated with this nanosized sample and activated carbon show much better rate capability, even at 100 C discharge rate, the hybrid capacitor also keeps 60% of capacity compared with 3C discharge rate.

Acknowledgments

Financial support from National Natural Science Foundation of China (no. 20373014) and the program of New Century Excellent Talents in University of China (2005) are acknowledged.

Fudan University assisted in meeting the publication costs of this article.

References

1. T. Ohzuku, Y. Iwakoshi, and K. Sawai, *J. Electrochem. Soc.*, **140**, 2490 (1993).
2. T. Ohzuku, A. Ueda, and N. Yamamoto, *J. Electrochem. Soc.*, **142**, 1431 (1995).
3. K. Zaghib, M. Armand, and M. Gauthier, *J. Electrochem. Soc.*, **145**, 3135 (1998).
4. A. N. Jansen, A. J. Kahaian, K. D. Kepler, P. A. Nelson, K. Amine, D. W. Dees, D. R. Vissers, and M. M. Thackeray, *J. Power Sources*, **81-82**, 902 (1999).
5. A. Guerfi, S. Sévigny, M. Lagacé, P. Hovington, K. Kinoshita, and K. Zaghib, *J. Power Sources*, **119-121**, 84 (2003).
6. K. Ariyoshi, S. Yamamoto, and T. Ohzuku, *J. Power Sources*, **119-121**, 959 (2003).
7. K. Nakahara, R. Nakajima, T. Matsushima, and H. Majima, *J. Power Sources*, **117**, 131 (2003).
8. P. Kubiak, A. Garcia, M. Womes, L. Aldon, J. O. Fourcade, P. E. Lippens, and J. C. Jumas, *J. Power Sources*, **119-121**, 626 (2003).
9. G. G. Amatucci, F. Badway, A. D. Pasquier, and T. Zheng, *J. Electrochem. Soc.*, **148**, A930 (2001).
10. A. D. Pasquier, I. Plitz, J. Gural, S. Menocal, and G. Amatucci, *J. Power Sources*, **113**, 62 (2003).
11. L. Kavan, J. Prochazka, T. M. Spittler, M. Kalbac, M. Zukalova, T. Drezzen, and M. Gratzel, *J. Electrochem. Soc.*, **150**, A1000 (2003).
12. W. Liu, G. C. Farrington, F. Chaput, and B. Dunn, *J. Electrochem. Soc.*, **143**, 879 (1996).
13. J. Lee, Y. W. Tsai, R. Santhanam, B. J. Hwang, M. H. Yang, and D. G. Liu, *J. Power Sources*, **119-121**, 721 (2003).
14. H. Gadjov, M. Gorova, V. Kotzeva, G. Avdeev, S. Uzunova, and D. Kovacheva, *J. Power Sources*, **134**, 110 (2004).
15. T. Doi, Y. Iriyama, T. Abe, and Z. Ogumi, *Chem. Mater.*, **17**, 1580 (2005).
16. W. Tang, H. Kanoh, and K. Ooi, *Electrochem. Solid-State Lett.*, **145-146**, 1 (1998).
17. X. Yang, W. Tang, H. Kanoh, and K. Ooi, *J. Mater. Chem.*, **9**, 2683 (1999).
18. C. Han, Y. Hong, C. M. Park, and K. Kim, *J. Power Sources*, **92**, 95 (2001).
19. H. Liang, X. Qiu, S. Zhang, Z. He, W. Zhu, and L. Chen, *Electrochem. Commun.*

- 6, 505 (2004).
20. C. Shen, X. Zhang, Y. Zhou, and H. Li, *Mater. Chem. Phys.*, **78**, 437 (2002).
21. M. Nakamichi, H. Kawamura, and M. Uchida, *Fusion Eng. Des.*, **69**, 257 (2003).
22. A. Guerfi, S. Sévigny, M. Lagacé, P. Hovington, K. Kinoshita, and K. Zaghbi, *J. Power Sources*, **119-121**, 88 (2003).
23. J. Li, Z. Tang, and Z. Zhang, *Electrochem. Commun.* **7**, 894 (2005).
24. T. Takada, H. Enoki, H. Hayakawa, and E. Akiba, *J. Electrochem. Soc.*, **139**, 290 (1998).
25. K. Ariyoshi, Y. Iwakoshi, N. Nakayama, and T. Obzuku, *J. Electrochem. Soc.*, **151**, A296 (2000).
26. D. L. Li, H. S. Zhou, and I. Honma, *Nat. Mater.*, **3**, 65 (2004).